Chemical Engineering Journal 146 (2009) 168–173

Contents lists available at ScienceDirect

Chemical Engineering Journal

journal homepage: www.elsevier.com/locate/cej

Review

Regeneration of acid orange 7-exhausted granular activated carbon with dielectric barrier discharge plasma

Guang-Zhou Qu, Jie Li*, Yan Wu, Guo-Feng Li, Duan Li

Institute of Electrostatics and Special Power, Dalian University of Technology, Dalian 116024, China

ARTICLE INFO

Article history:
Received 12 May 2007
Received in revised form 25 June 2008
Accepted 1 July 2008

Keywords:
Dielectric barrier discharge
Granular activated carbon
Acid orange 7
Functional groups
Adsorption kinetics
Adsorption equilibrium isotherms

ABSTRACT

A novel process for regenerating activated carbon based on high active species (O_3, $^{\bullet}OH$, $^{\bullet}HO_2$, $^{\bullet}O_2$ and $^{\bullet}RO$, etc.) generated by dielectric barrier discharge (DBD) oxidation was proposed. The method was assayed with granular activated carbon (GAC) exhausted with azo dye acid orange 7. The regeneration efficiency of this technique was evaluated, and the regeneration efficiencies could reach over 73% after five continuous regeneration cycles. The effects of DBD on the adsorption rate, the texture characteristic, the surface chemistry, and the adsorption capacity of GAC samples after different regeneration cycles were investigated. The adsorption rate remained stable after multi-successive regeneration cycles. The analysis of texture of GAC samples showed that the specific surface area and pore volume decreased after DBD regeneration cycles except for the first regeneration sample. It was observed that DBD also resulted in the increase of carboxylic functional groups of GAC's surface. Furthermore, all adsorption equilibrium isotherms fitted the Freundlich model fairly well, which demonstrated DBD plasma did not appear to modify adsorption process but to shift the equilibrium towards lower adsorption concentrations.

1. Introduction

Activated carbon (AC) has been widely used as an efficient and versatile adsorbent in the removal of gaseous pollutants, the treatment of waste water and the deep purification of drinking water due to their extended surface area, tailored pore distribution, and high degree of surface reactivity [1,2]. Commonly, when AC's adsorption capacity was exhausted, the spent AC should be regenerated because of the limited resources for AC production and additional secondary pollution of spent-carbon dumped into water or soil [3]. As a result, a wide variety of AC regeneration techniques, such as thermal regeneration [4,5], solvent regeneration [6], direct oxidation and catalytic wet oxidation regeneration [7,8] and biological regeneration [9], have been proposed and applied in past decades. But these techniques have a few disadvantages, for example, high temperature, high cost of the reagents employed and the danger from additional secondary pollution, and low regeneration efficiency, and so on. In recent years, more restrictive regulations on environmental protection and increased price of AC also have motivated researchers to develop new methods for regeneration and reuse of spent activated carbon [3,10]. Among them, microwave regeneration [11], electrochemical method [12], supercritical or subcritical WO regeneration [13,14] or ultrasonic regeneration [15] could be highlighted. Unfortunately, in most of the cases complicated processes were required for the implementation of the above mentioned methods.

In this paper, we reported on a novel AC regeneration method—dielectric barrier discharge (DBD) plasma regeneration. The DBD can produce non-thermal plasma under atmospheric pressure easily by applying high voltage to electrodes, one of which is at least covered with dielectric material. The plasma provides active species such as O_3, high-energy electron and various high oxidation potential free radicals [16], which might be effective for the oxidation of pollutants on AC. At present DBD techniques have been extensively used in environmental protection [17–20], and some experimental efforts also have been referred on the surface modification of activated carbons with DBD plasma [21,22]. However, to our knowledge, there were very few studies on the regeneration of AC with DBD plasma.

The objective of this study was to determine that the decomposition and desorption of contaminants from AC could be recovered to what extent after multi-successive DBD regeneration cycles. The effects of DBD on the adsorption rate, the regeneration efficiency, the texture characteristic, the surface chemistry and the adsorption capacity of AC samples were investigated in order to obtain some mechanisms involving in DBD plasma regeneration. The results were expected to provide some useful information as to regeneration of reactive dyes or other adsorbate-exhausted ACs with DBD plasma.

* Corresponding author. Fax: +86 411 84708576.
E-mail address: lijie@dlut.edu.cn (J. Li).

1385-8947/$ – see front matter © 2008 Elsevier B.V. All rights reserved.
doi:10.1016/j.cej.2008.07.007

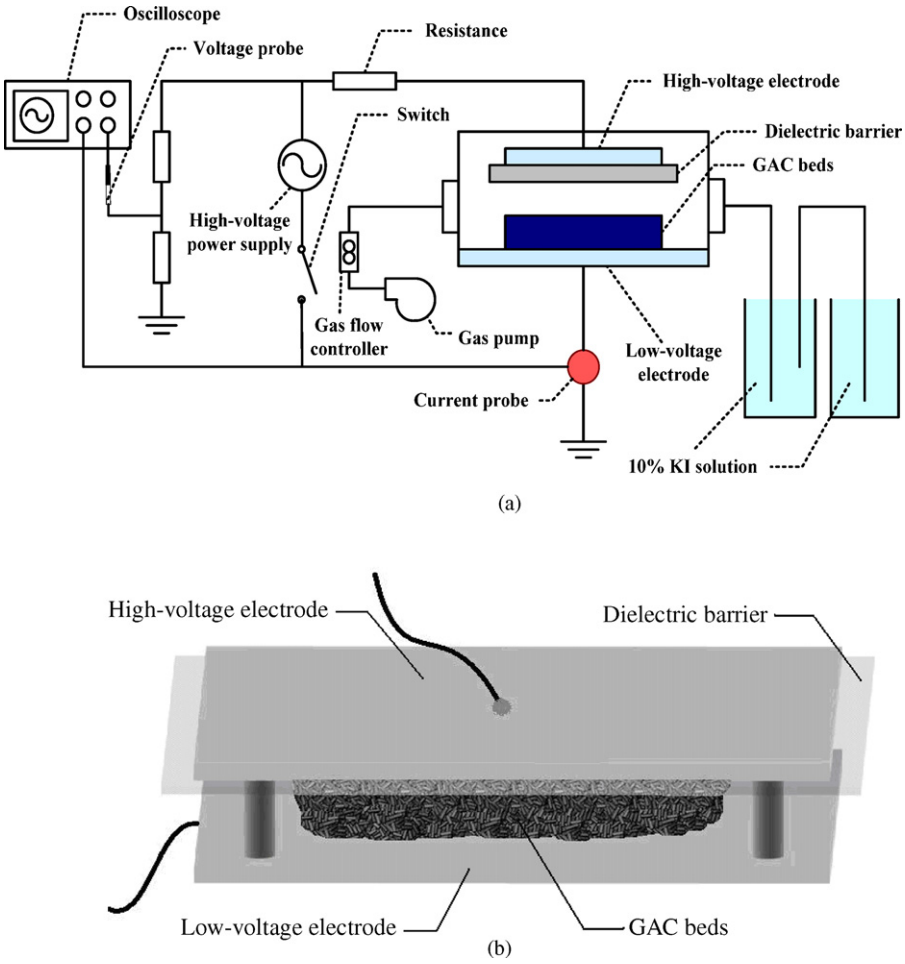

Fig. 1. Schematics of the experimental setup: (a) reaction system and (b) electrode structure of reactor.

2. Experimental

2.1. Materials

A commercial columned coal-based granular activated carbon (GAC, 4 mm diameter, 6–8 mm length, supplied by Gongyi Zhulin Filtrate Material Factory, China) was used as the adsorbent for experiments. As Quan et al. [11] described, prior to use, the GAC should be pretreated. Acid orange (AO7, purity greater than 98%) and distilled water were used to prepare the aqueous solutions for the tests in this study. The chemicals used for acid–base properties estimation were of analytical reagent grade and were obtained from Tianjin Kermel Chemical Reagent Co. Ltd. (Tianjin, China).

2.2. The DBD regeneration reaction system

The schematics of the experimental setup were given in Fig. 1. It mainly consisted of alternating current high-voltage power supply and DBD reactor. The frequency of alternating current high-voltage power supply of this experiment was 50 Hz, the voltage was 0–50 kV adjustable. Typical voltage and current waveforms delivered to the DBD reactor were recorded with the digital oscilloscope (Tektronix TDS2014, USA) with the help of a voltage probe (Tektronix P6021, USA) and a current probe (Tektronix P6021, USA) and shown in Fig. 2. The DBD experimental reactor was a parallelepiped Plexiglas chamber (450 mm × 400 mm × 120 mm), containing two rectangular parallel-plate electrodes made of stainless steel, the size of the two electrodes were 200 mm × 200 mm × 2 mm and 250 mm × 250 mm × 2 mm, respectively. The high-voltage electrode was covered by a 2 mm thick dielectric barrier (300 mm × 300 mm quartz glass plate, the dielectric constant, $\varepsilon = 7.0$). The gap space between the dielectric barrier and the low-voltage electrode was maintained at 15 mm. At terminal of the

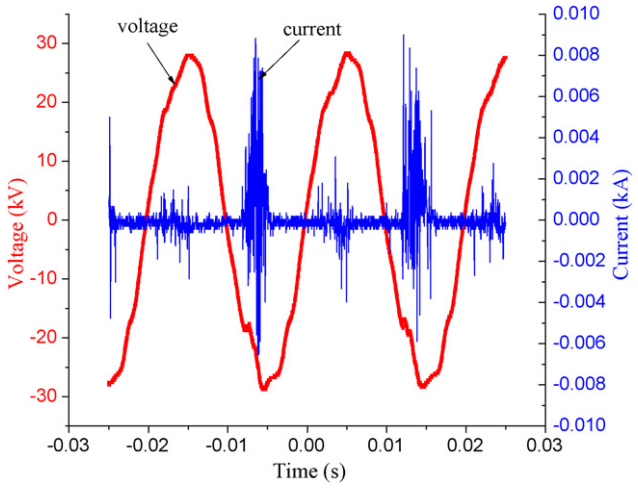

Fig. 2. Voltage and current waveforms delivered to the DBD regeneration reactor.

experiment setup, two bottles both containing 50 ml of 10% KI solution were used to collect distillate and exhaust gas.

2.3. The regeneration of GAC

As previously commented, the regeneration of spent AC was carried out in the DBD reactor mentioned above. Prior to regeneration, a known mass of prepared exhausted GAC, the moisture content was controlled at about 16%, was introduced into the reactor and was evenly spread over the low-voltage electrode's surface of the reactor (see b of Fig. 1). The regeneration of GAC began when the alternating current high-voltage power supply was turned on, and the regeneration would last for 180 min. In each regeneration experiment, the thickness of the GAC beds was kept at 4mm and the air was impregnated to the reactor with a flow rate of 0.01 m^3/min. Unless special conditions were required, all experiments were conducted at room temperature and atmospheric pressure.

2.4. Kinetics adsorption

The kinetics adsorption of AO7 on virgin and regenerated carbon was carried out in a rapid small-scale continuous cycle flow adsorption column (6 cm diameter and 20 cm length), where GAC sample was placed, AO7 solution (initial concentration 50 mg/l) was circulated through the adsorption column by a peristaltic pump at a flow rate of 160 ml/min. The residual concentration was continuously monitored by a UV–vis spectrophotometer (UV-2102C, Unico (Shanghai, China) Instrument Co., Ltd.) at the characteristic wavelength of 485 nm.

2.5. Adsorption equilibrium isotherms

Adsorption isotherms of AO7 aqueous solutions onto GAC samples were performed by the batch method in an end-over-end stirrer. Different amounts of carbon were added into different bottles containing 80 ml of AO7 aqueous solution of 1000 mg/l. The sealed bottles were shaken with a constant speed of 120 rpm at room temperature for 7 days. After the equilibrium reached, the suspensions were filtered and saved for further analysis. Quantitative analysis of the studied solutions was made based on the calibration curves of standard solutions, samples of 3 ml were withdrawn for analysis using UV–vis spectrophotometer to determine the concentration of AO7 remaining in the fluid phase, and the amounts of AO7 adsorbed onto the GAC were inferred from the mass balance as follows:

$$q_e = \frac{(C_0 - C_e)V}{m} \quad (1)$$

where q_e is the amount of AO7 per gram of adsorbent, V is the volume of the liquid phase, C_0 is the concentration of the solute in the bulk phase before it comes in contact with the adsorbent, C_e is the concentration of the solute in the bulk phase at equilibrium, and m is the amount of the adsorbent.

2.6. Analysis method

The structural properties of virgin and regenerated carbon were obtained from the physical adsorption of N_2 at 77 K determined by a Quantachrome autosorb-1 adsorption apparatus (Autosorb-1, Quantachrome Com. USA). The surface areas and pore size distributions (PSD) and total pore volume ($V_{Total\ pore}$) were calculated using the Langmuir equations and the Horvath–Kawazoe (HK) model [23], respectively. The micropore volume ($V_{Micropore}$), micropore area ($S_{Micropore}$) and external surface area ($S_{External}$) were obtained from the de Boer's t-plot method [24]. The surface chemistry of the GAC samples was examined by the determinations of pH value, basicity, acidity and various functional groups. The pH value of the GAC surface was evaluated according to ASTM standard procedure D 3838 [25], the basicity, acidity and various functional groups were measured using the titration method of Boehm [26].

3. Results and discussion

In this section, the discussion of the results obtained will focus on analyzing the effect of the carbon regeneration on: the adsorption kinetics, the regeneration efficiency, the textural characteristic and surface chemistry, and the adsorption capacity of carbon samples.

For convenience, the adsorption and subsequent regeneration process were considered as one regeneration cycle in this study, regenerated samples would be denoted as DBDi (i: the number of DBD regeneration cycle), for instance, sample DBD1 corresponds to one adsorption-DBD treatment cycle sample.

3.1. Effect of regeneration on the adsorption kinetics and regeneration efficiency

The effect of the regeneration treatment on the adsorption rate of the carbon samples were determined by analyzing of the decay curves of AO7 on the virgin and regenerated GACs.

The Fig. 3 showed the decay curves of AO7 onto different DBD regeneration GACs at different interval. It could be seen from the plots of the residual concentration versus t that the decay curves of the regenerated carbon were higher than that of the virgin carbon (VC), but after the third DBD regeneration cycles only a slight change in adsorption rate curves was noticed, which suggested that the adsorption rate remained stable after multi-successive regeneration cycles. Since the regeneration efficiency could reveal the effect of DBD plasma regeneration process, the regeneration yield was also calculated using the following equation

$$RE = \frac{q_r}{q_v} \times 100\% \quad (2)$$

where q_v is the adsorption capacity of VC, i.e. the equilibrium amount of contamination adsorbed per unit mass of AC (mg/g), and q_r is the adsorption capacity of regeneration carbon after the re-adsorption equilibrium.

All regeneration yields of this regeneration process in different regeneration cycles were presented in Fig. 4 and show that the

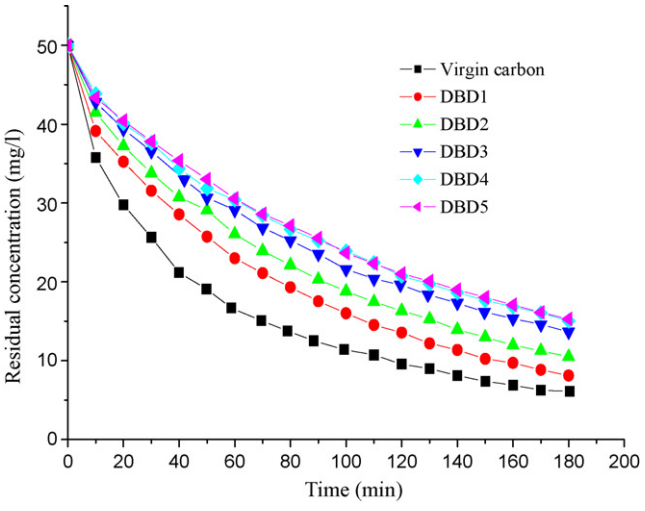

Fig. 3. Concentration decay curves for AO7 aqueous solutions on GAC samples.

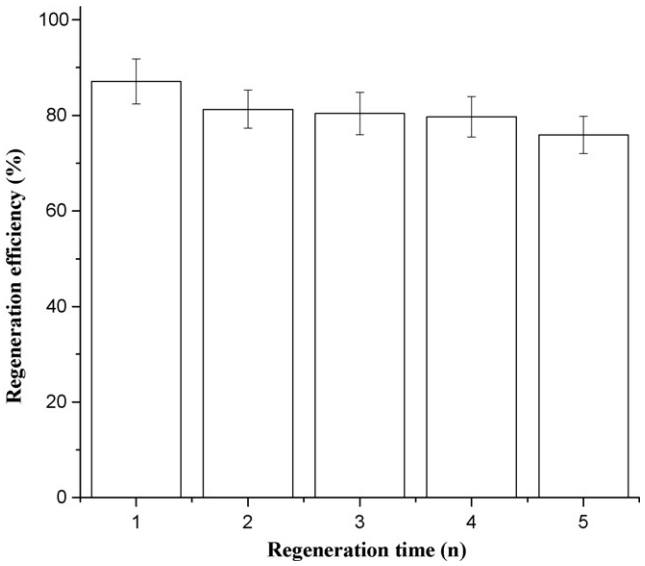

Fig. 4. The regeneration efficiencies of GACs after different DBD plasma regeneration cycle.

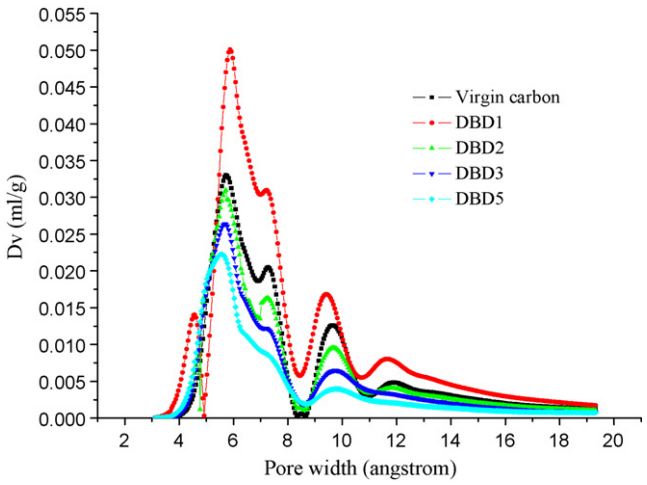

Fig. 5. Pore size distribution of virgin and DBD treated GAC by HK method.

recovery of regenerated GAC's capacity of adsorption was basically achieved. Even after five regeneration cycles, regeneration efficiencies of this technique were higher than 73%, and the decrease in regeneration efficiencies in successive regeneration cycles was small and almost were neglected except for the first regeneration of the fresh carbon. This result showed that the procedure still had a much greater efficiency after multi-successive regeneration cycles than that reported [27,28], and was a promising technique. Whereas, consistent with the adsorption rate, we also observed that the regeneration efficiencies decreased with regeneration cycles increasing, which will be explained by the changes of structural properties and surface chemistry of GAC samples after DBD plasma treatment (discussion below).

3.2. Effect of regeneration on the structural properties and surface chemistry of carbon

Table 1 mainly summarized relevant micropore structural properties of virgin and different regenerated GAC. According to the data presented in Table 1, it could be observed that the structural properties in DBD regeneration samples differed noticeably from those in the VC. After the first regeneration cycle, the sample had a larger Langmuir surface area ($S_{Langmuir}$), $S_{Micropore}$, $S_{External}$, $V_{Micropore}$ and $V_{Total\ pore}$ than the virgin sample. In subsequent regeneration cycles, the $S_{Langmuir}$, $S_{Micropore}$, $V_{Micropore}$, $S_{External}$ and $V_{Total\ pore}$ decreased with regeneration cycle increasing.

The PSD curves in micropore regions (micropores are defined as pores of width less than 2 nm) of GAC samples were also shown in Fig. 5. Evidently, with the increasing of regeneration cycle, the rules of pore size distribution were similar with that of $S_{Langmuir}$'s change.

Table 2
Acid–base properties of VC and DBD treated GACs (mmol/g)

Sample	pH	Carboxylic	Lactonic	Phenolic	Basic	Acidic	All groups
DBD_N[a]	2.28	0.242	0.307	0.296	0.108	0.845	0.953
VC	2.38	0.207	0.184	0.542	0.257	0.932	1.189
DBD1	2.44	0.227	0.262	0.309	0.218	0.798	1.016
DBD2	2.50	0.236	0.323	0.184	0.178	0.743	0.921
DBD3	2.32	0.269	0.069	0.485	0.113	0.822	0.935
DBD4	2.34	0.421	0.108	0.464	0.110	0.863	0.972
DBD5	2.30	0.447	0.155	0.412	0.061	1.014	1.075

[a] GAC sample of DBD treatment for 180 min in the absence of the adsorbate.

Comparing data in Table 1 and curves in Fig. 5, it could be inferred that the porosity of GAC was developed after one DBD plasma treatment, which might be owing to DBD plasma activation [29,30], while in subsequent regeneration cycles, the successive strong DBD process might cause wall destruction and pore blockage in the ranges of micropores [22].

According to above these results, the decrease of the adsorption rate of treated carbon samples and regeneration efficiency might be in part explained by wall destruction and pore blockage in the ranges of micropores. However, we also found that in spite of a significant increase of the specific surface area, pore volume after the first DBD treatment, the adsorption rate and regeneration efficiency of regenerated carbons were lower than that of VC, this should be related to the surface chemistry of the GACs except for a longer diffusion path of micropores would result in a greater probability for the pore blockage in the process of diffusion. Therefore, it was assumed that the surface chemistry of the GACs would experience some change during DBD.

Table 2 presented the results from the acid–base titrations of the virgin and generated carbon together with the pH of the GACs in aqueous solution. It could be seen from Table 2 that the pH values of the GAC samples assumed strong acidity, as it was mentioned above, which was due to pretreatment of hydrochloric acid to GAC.

Table 1
Structural properties of the VC and DBD treated GAC samples

GAC sample	$S_{Langmuir}$ (m^2/g)	$S_{Micropore}$ (m^2/g)	$S_{External}$ (m^2/g)	$V_{Micropore}$ (m^2/g)	$V_{Total\ pore}$ (m^2/g)	Average pore diameter (Å)
VC	594.9	346.9	66.9	0.1756	0.2899	9.8
DBD1	863.8	492.8	85.4	0.2509	0.3616	8.4
DBD2	573.4	312.9	63.8	0.1683	0.2731	9.5
DBD3	518.9	290.4	57.1	0.1468	0.2510	9.6
DBD5	459.2	246.8	51.6	0.1390	0.2173	9.5

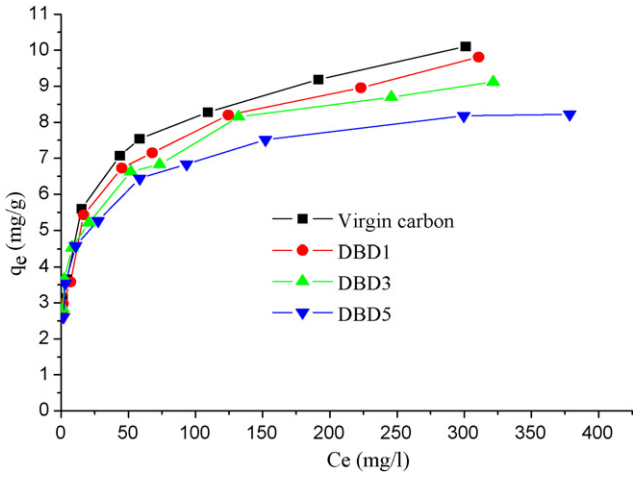

Fig. 6. Adsorption isotherms of AO7 on VC and different adsorption–DBD regeneration cycle GACs.

The differences in surface chemistry of the GAC samples were clearly seen from the Boehm titration results presented in Table 2. With the regeneration cycle increasing carboxylic on GAC samples increased, conversely, the basic decreased. It was interesting to note that the lactonic abrupt decreased after the second regeneration cycle, but in subsequent regeneration it increased with regeneration cycle increasing. Compared with the change trend of lactonic, the phenolic presents reverse change rule, after the second regeneration cycle, the phenolic groups of regenerated carbon were more than that of VC and again decreased as the regeneration cycles increasing. However, all groups had a slight change.

Though these results were currently not fully understood, it could be summarized that structural properties change, modification of DBD to GAC surface, and oxidation or incorporation of by-product from AO7 decomposition and desorption played an important role in changing of chemical surface groups.

To further confirm DBD plasma not only decomposed the adsorbed contaminants on GAC, but also changed the chemical characteristics of GAC itself, the surface chemistry of the GAC in the absence of the adsorbate with DBD plasma treatment was evaluated. The data in Table 2 (see DBD_N) showed that the functional groups of GAC sample treated in the absence of the adsorbate with DBD differed noticeably from those in the VC. It could concluded that DBD induced some acid groups onto GAC and changed to a great extent surface chemical characteristics of GAC itself, which also might be affirmed by the fact that basic of GAC treated in the absence of the adsorbate was less than that of VC.

Moreno-Castilla et al. [31] reported that the relative affinity of the phenolic compounds toward the surface of the activated carbon was related to the electron donor–acceptor complexes formed between the basic sites on the carbon surface (basic surface oxygen complexes and/or π electron-rich regions at the basal planes) and the aromatic ring. Thus, with carboxylic groups increasing of the carbon surface, the relative affinity weakens. These maybe indicate that the changes of chemical surface groups also could result in the decrease of adsorption rate of treated carbon and regeneration efficiency in a way.

3.3. *Effect of regeneration on adsorption capacity of carbon*

A simple comparison among adsorption isotherms done between virgin and different DBD regenerated GACs allows us to get average information about the effect of DBD on adsorption capacity. Fig. 6 showed the adsorption isotherms of virgin and different regenerated GAC, the isotherm for the first regeneration carbon was clearly located under that for VC, the isotherm for the third regeneration carbon was located in between the first and fifth regeneration carbon. We also observed that in spite of a significant increase of the specific surface area, pore volume after the first DBD treatment, the adsorption capacity of GAC did not reach its initial value, the value of q_e for the GAC samples decreased with the regeneration cycle increasing.

Table 3
Freundlich constants for adsorption of AO7 on GAC

Sample	K_F (l/g)	$1/n$	R^2
VC	2.91	0.23	0.99
DBD1	2.81	0.22	0.97
DBD3	2.89	0.20	0.99
DBD5	2.64	0.20	0.97

As the fractional coverage of the pore surface not only depends on surface area, pore size distribution, but also relates with the length of the diffusion path and surface chemistry and adsorption rate, and so on, so the specific surface area value itself is often not enough to determine the adsorption capacity of AC [1,32–34]. The porosity of GAC sample was developed after the first regeneration cycle, however, in the process of diffusion, a longer diffusion path of micropores would result in a greater probability for the pore blockage. As a result, the surface of the micropores could not be completely utilized in adsorption. On the other hand, we believed that the relative affinity weaken between adsobates and surface chemistry on GAC and AO7 in the bulk phase solution with the carboxylic groups increasing and the by-producted molecules or atoms polarized on regenerated carbon [31], the adsorptive rate also became slower after DBD treatment, thus, a smaller coverage. With regeneration cycle increasing, as it has been mentioned above, the GAC wall destruction, pore blockage and subdued relative affinity resulted in the decrease of adsorption capacity.

Another aspect that concerned us was the adsorption type of AO7 on carbon samples after DBD treatment, therefore, the Freundlich model was used in the adsorption isotherms above. Freundlich model is usually expressed by Freundlich equation as follows [33]:

$$q_e = K_F C_e^{1/n} \quad (3)$$

where q_e is the amount adsorbed at equilibrium, C_e is the equilibrium solution phase concentration, K_F (l/g) is the Freundlich parameter for a heterogeneous adsorbent, and the exponential term, $1/n$ (dimensionless), is related to the magnitude of the adsorption driving force and to the adsorbent site energy distribution.

Values of K_F (l/g) and $1/n$ (dimensionless) were calculated from the intercepts and slopes of the linear plots of $\ln q_e$ versus $\ln C_e$, and were listed in Table 3. The results suggested that all these isotherms well fitted with the Freundlich equation, similar observation was reported for the adsorption of AO7 on GAC [11]. It indicated that DBD did not appear to modify adsorption process but to shift the equilibrium towards lower adsorption concentrations. All n values were higher than 1 indicating favorable adsorption of AO7 onto GAC, as expected. This could be confirmed by the adsorption curves of AO7 on GAC (Fig. 6).

4. Conclusions

The results obtained in this study showed that the regeneration of spent granular carbon exhausted with AO7 by DBD plasma treatment was feasible. After multi-regeneration cycles, the adsorption rates for AO7 on GAC remained stable. It could be observed that

recovery of adsorption capacity was achieved ultimately. Even though experiencing five regeneration cycles, the regeneration efficiencies were higher than 73%. The DBD plasma not only decomposed the adsorbed contaminants on GAC, but also changed the texture and chemical characteristics of GAC itself. In spite of a significant increase of the specific surface area, pore volume after the first DBD treatment, the adsorption capacity of GAC did not reach its initial value, on the one hand, a longer diffusion path of micropores would result in a greater probability for the pore blockage in the process of diffusion, on the other hand, with carboxylic groups increasing and the by-product molecules or atoms polarized under stronger electric field on regenerated carbon, the relative affinity weaken between adsobates and surface chemistry on GAC and AO7 in the bulk phase solution. The adsorption isotherms well fitted with the Freundlich equation in all cases, which demonstrated DBD did not appear to modify adsorption process but to shift the equilibrium towards lower adsorption concentrations.

Acknowledgements

The authors are grateful for financial support provided by the Project Sponsored by the Scientific Research Foundation for the Returned Overseas Chinese Scholars, State Education Ministry.

References

[1] S. Yenisoy-Karakas, A. Aygün, M. Günes, E. Tahtasakal, Physical and chemical characteristics of polymer-based spherical activated carbon and its ability to adsorb organics, Carbon 42 (2004) 477–484.
[2] C.T. Hsieh, H. Teng, Influence of mesopore volume and adsorbate size on adsorption capacities of activated carbons in aqueous solutions, Carbon 38 (2000) 863–869.
[3] C.O. Ania, J.A. Menéndez, J.B. Parra, J.J. Pis, Microwave-induced regeneration of activated carbons polluted with phenol: a comparison with conventional thermal regeneration, Carbon 42 (2004) 1383–1387.
[4] M. Suzuki, D.M. Misic, O. Koyama, K. Kawazoe, Study of thermal regeneration of spent activated carbons: thermogravimetric measurement of various single component organics loaded on activated carbons, Chem. Eng. Sci. 33 (1978) 271–279.
[5] G. San-Miguel, S.D. Lambert, N.J.D. Graham, The regeneration of field spent activated carbons, Water Res. 35 (2001) 2740–2748.
[6] D. Chinn, C.J. King, Adsorption of glycols, sugar, and related multiple-OH compounds onto activated carbons. 2. Solvent regeneration, Ind. Eng. Chem. Res. 38 (1999) 3746–3753.
[7] J.F. González, J.M. Encinar, A. Ramiro, E. Sabio, Regeneration by wet oxidation of an activated carbon saturated with *p*-nitrophenol, Ind. Eng. Chem. Res. 41 (2002) 1344–1351.
[8] S. Moshe, I. Yurii, M. Matatov, Comparison of catalytic processes with other regeneration methods of activated carbon, Catal. Today 53 (1999) 73–80.
[9] M. Scholz, R.J. Martin, Control of bio-regenerated columned granular activated carbon by spreadsheet modeling, J. Chem. Technol. Biot. 71 (1998) 253–261.
[10] S.H. Lin, M.J. Cheng, Adsorption of phenol and *m*-chlorophenol on organobentonites and repeated thermal regeneration, Waste Manage 22 (2002) 595–603.
[11] X. Quan, X.T. Liu, L.L. Bo, S. Chen, Y.Z. Zhao, X.Y. Cui, Regeneration of acid orange 7-exhausted columned granular activated carbons with microwave irradiation, Water Res. 38 (2004) 4484–4490.
[12] R.M. Narbaitz, J. Cen, Electrochemical regeneration of columned granular activated carbon, Water Res. 28 (1994) 1771–1778.
[13] R.P. De Filippi, V.J. Krukonis, R.J. Robey, Model Supercritical Fluid Regeneration of Activate Carbon for Adsorption of Pesticides, Washington, DC, USA, EPA R600/2-80-054, 1980.
[14] F. Salvador, C. Sánchez Jiménez, A new method for regenerating activated carbon by thermal desorption with liquid water under subcritical conditions, Carbon 34 (1996) 511–516.
[15] O. Hamdaoui, E. Naffrechoux, J. Suptil, C. Fachinger, Ultrasonic desorption of *p*-chlorophenol from columned granular activated carbon, Chem. Eng. J. 106 (2005) 153–161.
[16] M.J. Kirkpatrick, Plasma-catalyst interactions in treatment of gas phase contaminants and in electrical discharge in water, The Florida State University, Dissertation, 2004 (Chapter I. Introduction).
[17] C. Subrahmanyam, M. Magureanu, A. Renken, L. Kiwi-Minsker, Catalytic abatement of volatile organic compounds assisted by non-thermal plasma. Part 1. A novel dielectric barrier discharge reactor containing catalytic electrode, Appl. Catal. B: Environ. 65 (2006) 150–156.
[18] I. Nagao, M. Nishida, K. Yukimura, S. Kambara, T. Maruyama, NOx removal using nitrogen gas activated by dielectric barrier discharge at atmospheric pressure, Vacuum 65 (2002) 481–487.
[19] S.L. Park, J.D. Moon, S.H. Lee, S.Y. Shin, Effective ozone generation utilizing a meshed-plate electrode in a dielectric-barrier discharge type ozone generator, J. Electrostat. 64 (2006) 255–262.
[20] R.B. Zhang, Y. Wu, J. Li, G.F. Li, Z.G. Zhou, Water treatment by biopolar pulsed dielectric barrier discharge in water–air mixture, J. Adv. Oxid. Technol. 7 (2004) 172–177.
[21] S. Kodama, H. Habaki, H. Sekiguchi, J. Kawasaki, Surface modification of adsorbents by dielectric barrier discharge, Thin Solid Films 407 (2002) 151–155.
[22] D. Lee, S.H. Honga, K.H. Paek, W.T. Ju, Adsorbability enhancement of activated carbon by dielectric barrier discharge plasma treatment, Surf. Coat. Technol. 200 (2005) 2277–2282.
[23] G. Horvath, K. Kawazoe, Method for the calculation of effective pore size distribution in molecular sieve carbon, J. Chem. Eng. Jpn. 16 (1983) 470–475.
[24] J.H. de Boer, B.C. Lippens, B.G. Linsen, J.C.P. Broekhoff, A. van den Heuvel, Th.J. Osinga, The *t*-curve of multimolecular N_2-adsorption, J. Colloid Interf. Sci. 21 (1966) 405–414.
[25] ASTM Annual Book of ASTM standards. Standard test method for pH of activated carbon, D3838-80, vol. 15.01, Philadelphia, PA, 1996, pp. 531–532.
[26] H.P. Boehm, Surface oxides on carbon and their analysis: a critical assessment, Carbon 40 (2002) 145–149.
[27] P.C. Chiang, E.E. Chang, J.S. Wu, Comparison of chemical and thermal regeneration of aromatic compounds on exhausted activated carbon, Wat. Sci. Technol. 35 (1997) 179–185.
[28] H.P. Zhang, Regeneration of exhausted activated carbon by electrochemical method, Chem. Eng. J. 85 (2002) 81–85.
[29] C.Q. Wang, X.N. He, Preparation of hydrophobic coating on glass surface by dielectric barrier discharge using a 16 kHz power supply, Appl. Surf. Sci. 252 (2006) 8348–8351.
[30] C. Liu, R.D. Arnell, A.R. Gibbons, S.M. Green, L. Ren, J. Tong, Surface modification of PTFE by plasma treatment, Surf. Eng. 16 (2000) 215–217.
[31] C. Moreno-Castilla, J. Rivera-Utrilla, M.V. Lopez-Ramon, F. Carrasco-Marin, Adsorption of some substituted phenols on activated carbons from a bituminous coal, Carbon 33 (1995) 845–851.
[32] A. Kumar, S. Kumar, S. Kumar, Adsorption of resorcinol and catechol on granular activated carbon: equilibrium and kinetics, Carbon 41 (2003) 3015–3025.
[33] G.M. Walker, L.R. Weatherley, Adsorption of dyes from aqueous solution—the effect of adsorbent pore size distribution and dye aggregation, Chem. Eng. J. 83 (2001) 201–206.
[34] T. Karanfil, J.E. Kilduff, Role of granular activated carbon surface chemistry on the adsorption of organic compounds. 1. Priority pollutants, Environ. Sci. Technol. 33 (1999) 3217–3224.